

CHARACTERIZATION OF TURBULENT PROCESSES BY THE RAMAN LIDAR SYSTEM BASIL IN THE FRAME OF THE HD(CP)² OBSERVATIONAL PROTOTYPE EXPERIMENT – HOPE

Paolo Di Girolamo^{1*}, Donato Summa¹, Dario Stelitano¹, Marco Cacciani², Andrea Scoccione²,
Andreas Behrendt³, Volker Wulfmeyer³

¹*Scuola di Ingegneria, Università degli Studi della Basilicata, Viale dell'Ateneo Lucano n. 10, 85100 Potenza – Italy, *Email: digirolamo@unibas.it*

²*Dipartimento di Fisica, Università di Roma “Sapienza”, Piazzale Aldo Moro, n. 2, 00100 Roma – Italy*

³*Institut fuer Physik und Meteorologie, Universitaet Hohenheim, Hohenheim – Germany*

ABSTRACT

Measurements carried out by the Raman lidar system *BASIL* are reported to demonstrate the capability of this instrument to characterize turbulent processes within the Convective Boundary Layer (CBL). In order to resolve the vertical profiles of turbulent variables, high resolution water vapour and temperature measurements, with a temporal resolution of 10 sec and a vertical resolution of 90 and 210 m, respectively, are considered. Measurements of higher-order moments of the turbulent fluctuations of water vapour mixing ratio and temperature are obtained based on the application of spectral and auto-covariance analyses to the water vapour mixing ratio and temperature time series. The algorithms are applied to a case study (IOP 5, 20 April 2013) from the HD(CP)² Observational Prototype Experiment (HOPE), held in Central Germany in the spring 2013. The noise errors are demonstrated to be small enough to allow the derivation of up to fourth-order moments for both water vapour mixing ratio and temperature fluctuations with sufficient accuracy.

1. INTRODUCTION

Measurements of higher-order moments of moisture and temperature fluctuations provide unique and essential information for the characterization of turbulent processes within the convective boundary layer (CBL). Water vapour variance is a key parameter in many turbulence, convection, and cloud parameterizations. Within the CBL, water vapour variance increases with height, achieving a maximum at the top of the CBL due to the mixing of moist air in the updrafts with the drier air from above the CBL ([1];[2]).

Moreover, water vapour skewness and kurtosis are found to be characterized by an appreciable vertical variability within the CBL, which changes patterns during different phases of the CBL evolution.

Lidar systems, based on their capability to provide high space and time resolution and accurate measurements of atmospheric water vapour and temperature, have nowadays reached the level of maturity needed to investigate the relevant atmospheric processes and enable measurements of turbulent variables within the CBL (among others, [3] [4]). The major advantage of the lidar techniques is represented by its capability to characterize turbulent variables from the proximity of the surface up to interfacial layer and above.

In the present paper we report what we believe are the first simultaneous and co-located measurements of water vapour and temperature turbulent fluctuations performed by a single lidar system. These measurements have been carried out by the Raman lidar system *BASIL* exploiting its capability to perform high-resolution and accurate measurements of atmospheric temperature and water vapour, both in daytime and night-time, based on the application of the rotational and vibrational Raman lidar techniques in the UV, respectively ([5];[6]). Measurements of turbulent variables throughout the CBL by water vapour Raman lidar had been demonstrated to be possible by Wulfmeyer *et al.* [7] based on the use of the data from the Atmospheric Radiation Measurement (ARM) Raman lidar. However, these authors came to the conclusion that the noise errors affecting the ARM Raman lidar water vapour mixing ratio measurements are too large to derive fourth-order moments with sufficient

accuracy. Thus, to the best of our knowledge, *BASIL* is the first Raman lidar with a demonstrated capability to retrieve daytime profiles of water vapour turbulent fluctuations up to the fourth order throughout the atmospheric CBL, this capability being combined with the one to also measure daytime profiles of temperature fluctuations up to the fourth order.

2. METHODOLOGY

BASIL is a ground-based Raman Lidar hosted in a transportable sea-tainer. The major feature of *BASIL* is represented by its capability to perform high-resolution and accurate measurements of atmospheric temperature and water vapour, both in daytime and night-time, based on the application of the rotational and vibrational Raman lidar techniques in the UV. Besides temperature and water vapour, *BASIL* is also capable of providing measurements of particle backscatter at 355, 532 and 1064 nm, particle extinction at 355 and 532 nm and particle depolarization at 355 and 532 nm ([8]).

The accuracy of the measurements performed by *BASIL* is high enough to allow the retrieval of vertical profiles throughout the atmospheric CBL of the two turbulent variables (namely, water vapour mixing ratio and temperature) up to the fourth order during daytime. Results from this system are obtained based on the application of the approach introduced by Lenschow et al. [9], which allows to estimate higher-order moments of turbulent variables in the presence of noisy data.

As the atmospheric variance and the noise variance a measured atmospheric variable are uncorrelated, the total variance Var_m can be expressed as [9] $Var_m = Var_a + Var_n$, with Var_a being the atmospheric variance and Var_n being the noise variance.

Different procedures may be considered to separate atmospheric variance from the noise variance in the total measured variance. The auto-covariance method is probably the most effective and straightforward among these procedures. This method is based of the consideration that atmospheric fluctuations are correlated in time, while instrumental noise fluctuations are uncorrelated [9]. This approach determines the atmospheric variance based on the computation of the auto-covariance function for the considered

atmospheric variable and then extrapolating this function to zero lag based on the application of a power-law fit. As specified in Lenschow *et al.* [9], the auto-covariance function at zero lag represents the total measured variance and, consequently, the noise variance can be determined as the difference between the auto-covariance function extrapolated to zero lag and its value at zero lag.

3. RESULTS

In the selection of the case study to be included in this work, attention was paid on identifying weather conditions characterized by the presence of a consolidated, well-mixed and quasi-stationary CBL. Typically time segments with a duration of 1-2 hours are considered as in fact for longer periods the CBL can no longer be considered as being quasi-stationary, while the consideration of shorter periods would reduce the number of sampled thermals and thus increase the sampling errors.

Figure 1 illustrates the time-height plot of the particle backscatter coefficient at 1064 nm, $\square\beta_{par}$, between 11:30 and 13:30 UTC, on 20 April 2013, revealing the presence of a significant boundary layer aerosol loading (with values of $\square\beta_{par}$ in excess of $2 \times 10^{-5} \text{ m}^{-1} \text{ sr}^{-1}$), which testifies the presence of a well-mixed and quasi-stationary CBL at this time of the day, extending up to a height of approximately 1300 m. The figure reveals the alternation of updrafts associated with thermals of warm air rising from the ground and downdrafts associated with thermals of cool air sinking from the free troposphere. The evolution of z_i (black line in figure 1), determined with a conventional approach based on the detection of the strongest gradient of the aerosol backscatter signal, is found to be characterized by a limited time variability, with a mean value during the observation period of 1290 m a.g.l and a standard deviation of 77 m.

Figure 2 illustrates the time-height cross section of the water vapour mixing ratio (upper panel) and temperature (lower panel) in the same time interval considered in figure 1. The upper panel of figure 3 reveals the variability of the water vapour mixing ratio within the CBL associated with the presence of alternating updrafts and downdrafts. The largest variability is observed in the interfacial layer, which is characterized by the

penetration of the warm humid air rising from the ground and the entrainment of cool dry air sinking from the free troposphere. As for water vapour, the largest variability temperature profile (lower panel of figure 2) is observed in the interfacial layer, possibly as a result of sensible heat entrainment fluxes.

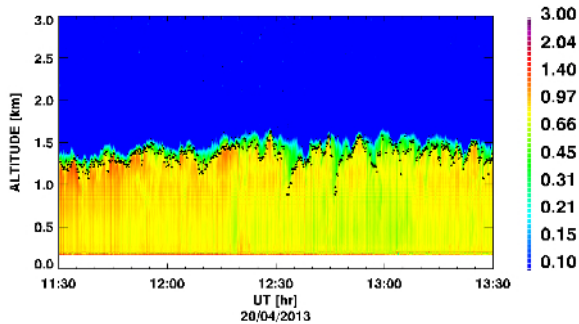


Figure 1: Time-height cross-section of β_{par} between 11:30 and 13:30 UTC on 20 April 2013. The black line in the figure identifies the CBL height z_i .

In order to characterize the quality of water vapour mixing ratio and temperature measurements, an accurate assessment of noise error profiles is necessary. Profiles of noise error affecting water vapour mixing ratio and temperature measurements are illustrated in figure 3, this being quantified as the root-square of the noise variance. For the vertical and temporal resolution selection considered for the turbulence measurements, i.e. 90 m/200m and 10 s, respectively, the statistical error affecting water vapour mixing ratio measurements is smaller than 0.06 g/kg up to 1.4 km, while the statistical error affecting temperature measurements is smaller than 2 K up to 1.3 km.

Figure 4 shows the vertical profiles of atmospheric and total variance for water vapour mixing ratio (upper panel) and temperature (lower panel). A maximum of the water vapour mixing ratio variance profile is observed in the interfacial layer at 1260 m, i.e. $0.29 \text{ g}^2/\text{kg}^2$ with $0.013 \text{ g}^2/\text{kg}^2$ and $0.032 \text{ g}^2/\text{kg}^2$ for the sampling error and noise error, respectively. The near-zero values in the lower CBL indicate weak surface forcing. In the interfacial layer, the variance reaches a maximum as a result of the large variability produced by the vertical exchange associated with the strong updrafts and downdrafts [9]. For what concerns

the temperature variance, a maximum of 0.4 K^2 is observed at 1310 m. Larger values of the temperature variance in the interfacial layer are the result of entrainment [1].

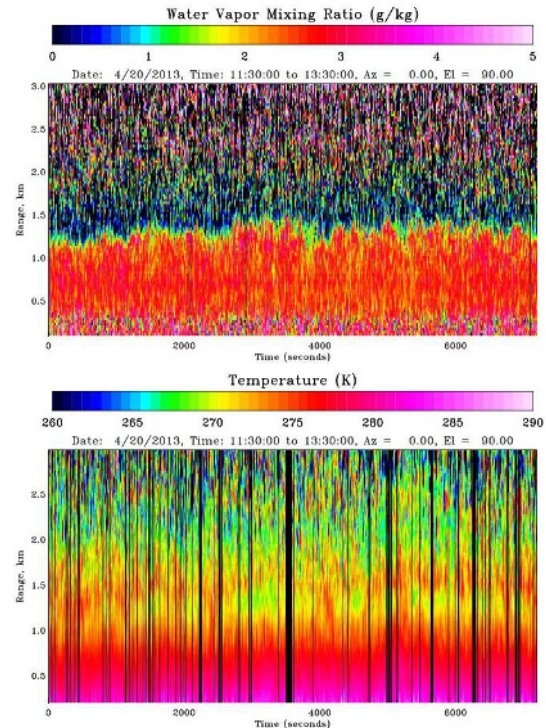


Figure 2: Time-height cross section of water vapour mixing ratio (upper panel) and temperature (lower panel) in the same time interval considered in figure 1.

Vertical profiles of the third-order moment for water vapour mixing ratio and temperature have also been determined, but are not shown here and will be illustrated at the Conference. Values of the third order moment of water vapour mixing ratio fluctuations are found to be negative between 900 and 1290 m, with a negative peak value of $-0.029 \pm 0.005 \text{ g}^3/\text{kg}^3$ at 1140 m, while a large positive peak is observed just above CBL top, with a maximum of $0.156 \pm 0.009 \text{ g}^3/\text{kg}^3$ at 1380 m. The third order moment of temperature fluctuations is characterized by a peak of $-0.11 \pm 0.01 \text{ K}^3$ around the top of the CBL at 1280 m. Water vapour mixing ratio fourth-order moment, also determined but not shown here, is almost zero up to $\cong 750 \text{ m}$ (i.e. $z/z_i = 0.6$), is characterized by a maximum of $0.28 \pm 0.13 \text{ g}^4/\text{kg}^4$ around the top of the CBL (at 1350 m), while temperature fourth-order moment, also not shown,

shows a maximum of $0.36 \pm 0.10 \text{ K}^4$ around the top of the CBL (at 1310 m).

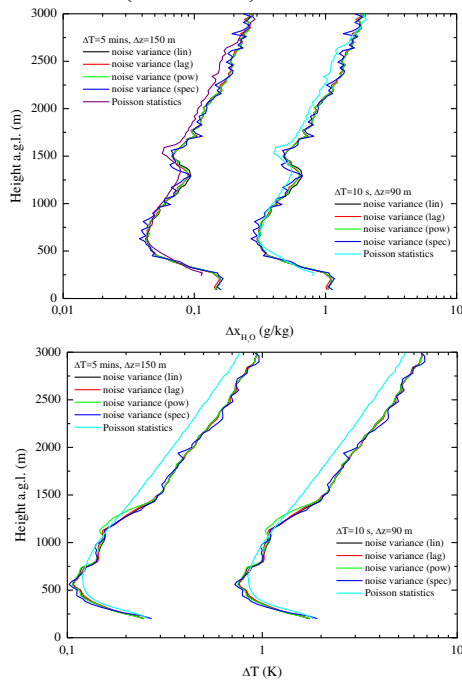


Figure 3: Profiles of noise error affecting water vapour mixing ratio (upper panel) and temperature (lower panel) measurements.

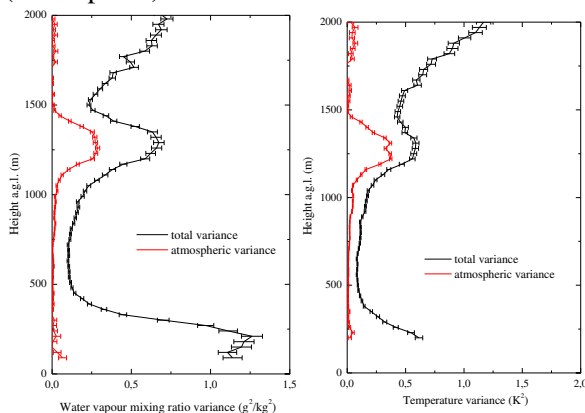


Figure 4: Vertical profiles of atmospheric and total variance for water vapour mixing ratio (left panel) and temperature (right panel).

4. CONCLUSIONS

This paper provides a detailed characterization of the performances of the Raman lidar *BASIL* and demonstrates that profiles of turbulent variables can be determined throughout the CBL with sufficient accuracy. For this purpose measurements from the HD(CP)2 Observational Prototype Experiment (HOPE), held in Central Germany in the spring 2013, are considered.

REFERENCES

- [1] Wulfmeyer, V., 1999: Investigation of turbulent processes in the lower troposphere with water-vapour DIAL and radar-RASS, *J. Atm. Sci.*, **56**, 1055–1076.
- [2] Wulfmeyer, V., 1999: Investigations of humidity skewness and variance profiles in the convective boundary layer and comparison of the latter with large eddy simulation results, *J. Atm. Sci.*, **56**, 1077–1087.
- [3] Frehlich, R., L. Cornman, 2002: Estimating spatial velocity statistics with coherent Doppler lidar, *J. Atmos. Ocean. Tech.*, **19**, 355–366.
- [4] Behrendt, A., V. Wulfmeyer, E. Hammann, S. K. Muppa, and S. Pal: 2014, Profiles of second- to third-order moments of turbulent temperature fluctuations in the convective boundary layer: first measurements with Rotational Raman Lidar", *Atmos. Chem. Phys. Discuss.*, **14**, 29019-29055.
- [5] Di Girolamo, P., R. Marchese, D. N. Whiteman, B. B. Demoz, 2004: Rotational Raman Lidar measurements of atmospheric temperature in the UV. *Geophys. Res. Lett.*, **31**, doi: 10.1029/2003GL018342.
- [6] Di Girolamo, P., D. Summa, R. Ferretti, 2009: Multiparameter Raman Lidar Measurements for the Characterization of a Dry Stratospheric Intrusion Event, *J. Atmos. Ocean. Tech.*, **26**, 1742-1762.
- [7] Wulfmeyer, V., D. D. Turner, S. Pal, E. Wagner, 2010: Can water vapour raman lidar resolve profiles of turbulent variables in the convective boundary layer ?, *Bound.-Lay. Meteorol.*, doi:10.1007/s10546-010-9494-z.
- [8] Di Girolamo, P., D. Summa, R. Bhawar, T. Di Iorio, M. Cacciani, I. Veselovskii, O. Dubovik, A. Kolgotin: 2012, Raman lidar observations of a Saharan dust outbreak event: Characterization of the dust optical properties and determination of particle size and microphysical parameters, *Atm. Env.*, **50**, 66-78.
- [9] Lenschow, D. H., V. Wulfmeyer., C. Senff, 2000: Measuring second-through fourth-order moments in noisy data. *J. Atmos. Ocean. Tech.*, **17**, 1330–1347.